

Article

# Parametric Design to Maximize Solar Irradiation and Minimize the Embodied GHG Emissions for a ZEB in Nordic and Mediterranean Climate Zones

Mattia Manni <sup>1</sup>, Gabriele Lobaccaro <sup>2,\*</sup>, Nicola Lolli <sup>3</sup> and Rolf Andre Bohne <sup>2</sup>

<sup>1</sup> Department of Engineering, CIRIAF—Interuniversity Research Center on Pollution and Environment “Mauro Felli”, University of Perugia, 06125 Perugia, Italy; manni@crbnet.it

<sup>2</sup> Department of Civil and Environmental Engineering, Faculty of Engineering, Norwegian University of Science and Technology, 7491 Trondheim, Norway; rolf.bohne@ntnu.no

<sup>3</sup> SINTEF Community—Architecture, Materials, and Structures, 7491 Trondheim, Norway; nicola.lolli@sintef.no

\* Correspondence: gabriele.lobaccaro@ntnu.no; Tel.: +47-918-13-568

Received: 4 August 2020; Accepted: 15 September 2020; Published: 22 September 2020



**Abstract:** This work presents a validated workflow based on an algorithm developed in Grasshopper to parametrically control the building’s shape, by maximizing the solar irradiation incident on the building envelope and minimizing the embodied emissions. The algorithm is applied to a zero-emission building concept in Nordic and Mediterranean climate zones. The algorithm enables conducting both energy and environmental assessments through *Ladybug* tools. The emissions embodied in materials and the solar irradiation incident on the building envelope were estimated in the early design stage. A three-steps optimization process through evolutionary solvers, such as Galapagos (one-objective) and Octopus (multi-objective), has been conducted to shape the most environmentally responsive ZEB model in both climates. The results demonstrated the replicability of the algorithm to optimize the solar irradiation by producing an increment of solar incident irradiation equal to 35% in the Mediterranean area, and to 20% in the Nordic climate. This could contribute to compensate the additional 15% of emissions due to the higher quantities of employed materials in the optimized design. The developed approach, which is based on the parametric design principles for ZEBs, represents a support instrument for designers to develop highly efficient energy solutions in the early design stages.

**Keywords:** life cycle assessment; zero-emission building; parametric design; evolutionary computing; solar irradiation

## 1. Introduction

The environmental impact of buildings on the global energy demand and atmospheric greenhouse gas (GHG) emissions has rapidly increased during recent decades. According to the Intergovernmental Panel on Climate Change (IPCC) [1], the building sector is responsible for over 40% of the global energy consumption and 18% of GHG emissions. The Fifth Assessment Report of IPCC describes buildings as a critical issue in the low-carbon energy transition and a global challenge to a sustainable development. Current technology in the building industry offers already available and highly cost-effective solutions to achieve a considerable reduction in energy demand and GHG emissions. In recent decades, the regulations and national building standards have focused on lowering the operational energy consumption [2–4]. In the Energy Roadmap 2050 published by the European Climate Foundation, five de-carbonization scenarios were proposed and these highlighted the importance of having an efficient use of on-site renewable energy sources (RES) [5]. In response to that, the concepts of net

zero-energy buildings (NZEB) and zero-emission buildings (ZEB) were developed to face the challenges of reducing energy consumption and GHGs, and increasing the on-site production of energy from RES.

The paper is structured as follows. The Background (Section 2) is articulated around three sub-sections describing the main research topics (Sections 2.1–2.3). The Methodology (Section 3) is divided into two sub-sections: in the first sub-section, the workflow is presented, while in the second sub-section, the case study is described (Sections 3.1 and 3.2). In the Results and Discussion (Section 4), the outcomes referring to the reference model, the exposure optimization process, and the responsive ZEB for each climate zone (Sections 4.1–4.3) are presented and discussed, then the evolutionary process is outlined (Section 4.4) and the limitations of the study are highlighted (Section 4.5). Finally, the Conclusions and Future Developments summarize the resulting knowledge generated and the implications of this work (Section 5).

## 2. Background

### 2.1. Towards GHGs Reduction: Zero-Emission Buildings

An NZEB is defined as a building with high energy efficiency, which can generate on-site as much energy from RES as it needs to cover its operational energy consumption on an annual basis. In that regard, relevant contributions to its definitions [6–8] are here included, such as the work done in the framework of the International Energy Agency (IEA) “Solar Heating and Cooling (SHC) Task 40 Net Zero Energy Solar Buildings”, in which the state of the art of zero-energy buildings and their classifications have been provided. Up to 30 net zero-energy buildings worldwide were analyzed and monitored for at least 12 months to define the best practices and develop design guidelines [9–13]. Other definitions of net zero-energy buildings are in the study conducted by Marszal et al. [14]. Methodologies for calculating the performance of ZEBs are described in the same research by integrating aspects of the life cycle assessments (LCA), as in [15,16]. The work conducted by Torcellini et al. [8] proposed a different categorization of ZEBs into four clusters based on boundary conditions, performance, and metrics. In Lund et al. [17], the ZEBs are grouped according to energy demand and installed systems for energy production.

The ZEBs implement both passive and active strategies. The use of RES and their integration on building components is rapidly growing worldwide [18]. The data reported from the IEA showed that the total installed production capacity of photovoltaic systems (PV) has grown with an average rate of 49% per year during the last ten years [19], and, similarly, an increment of 12% per year has been registered for solar thermal (ST) plants [20]. Furthermore, the growing interest toward bioclimatic and solar houses is demonstrated by numerous studies on the exploitation of solar irradiation for passive strategies [21–26]. The concept of a zero-emission solar house (ZESH) was proposed by Oliveira et al., 2017 [27], who developed the *Ekó House* ZEB concept, starting from the aforementioned classification proposed by Torcellini et al. [8].

This study aims at proposing a new parametric approach to optimize a ZEB residential design in the early design stage. The optimization strategies are pursued by maximizing the solar energy potential and minimizing the embodied emissions in the construction stage. The workflow is based on an algorithm for the multi-objective optimization of passive and active strategies and real-time evaluation of embodied and operational emissions. This workflow was tested in both Mediterranean and Nordic climate zones.

## 2.2. Parametric Design for Multi-Objective Optimization

The parametric-driven approach allows multi-objective optimization processes to define the optimized building shape configurations, simultaneously and automatically. Similar approaches have been adopted in other studies (Table 1). The research conducted by Yun Kyu [28] proposed a method to represent building geometry by implementing agent points (nodes), and showing a novel solution for building geometry construction. Such a workflow leads to design more energy-efficient buildings, with a better exploitation of solar radiation impinging on the building envelope. A similar approach has been developed by Lobaccaro [29]. By contrast, the study carried out by Zani [30] described a generative algorithm for handling varying hypotheses on user occupancy that can influence building energy performance.

**Table 1.** Overview of the existing workflows related to the parametric design for multi-objective optimization.

Authors	Reference	Year	Location	Case Study	Input *					Tools	Output **				Visualization	
					Wd	Gd	Mp	En	Lce		Ee	Oe	Irr	Df	3D	Graphs
Yun Kyu et al.	[28]	2009	USA	Single-family house	✓	✓	✓	✓	—	Excel	—	✓	✓	—	✓	—
Lobaccaro et al.	[29]	2016	Trondheim	Row houses	✓	✓	—	—	—	Rhinoceros; Grasshopper	✓	✓	✓	—	✓	—
Zani et al.	[30]	2017	Italy	University campus	✓	✓	✓	✓	—	Sketchup; Rhinoceros; Grasshopper; Ladybug; Honeybee; EnergyPlus; Octopus	—	✓	✓	—	✓	—
Kiss et al.	[31]	2020	Hungary	Generic building	✓	✓	✓	✓	✓	Rhinoceros; Grasshopper	✓	✓	—	—	✓	✓
Soflaei et al.	[32]	2020	USA	Courtyard housing	✓	✓	✓	✓	—	Rhinoceros; Grasshopper	—	—	✓	✓	✓	✓
Mahdavi Adeli et al.	[33]	2020	Iran	Single-family house	✓	✓	✓	✓	✓	Design Builder	✓	✓	—	—	—	✓
Lolli et al.	[34]	2017	Norway	ZEB residential single-family house	✓	✓	✓	✓	✓	Excel	✓	✓	—	—	—	✓

Table 1. Cont.

Authors	Reference	Year	Location	Case Study	Input *					Tools	Output **				Visualization	
					Wd	Gd	Mp	En	Lce		Ee	Oe	Irr	Df	3D	Graphs
Lobaccaro et al.	[35]	2018	Norway	Single-family house	✓	✓	✓	✓	✓	Rhinoceros; Grasshopper; DIVA for Gh; Ladybug; EnergyPlus; Octopus	✓	✓	✓	✓	✓	✓
Hollberg et al.	[36]	2016	Germany	Single-family house	✓	✓	✓	✓	✓	Rhinoceros; Grasshopper	✓	✓	—	—	✓	✓
Cavalliere et al.	[37]	2019	Switzerland	Generic building	—	✓	✓	—	✓	BIM	✓	—	—	—	—	✓
Ramin et al.	[38]	2019	Iran	Generic envelope	✓	✓	✓	✓	✓	N/A	✓	✓	—	—	—	✓
Azzouz et al.	[39]	2017	UK	Office building	✓	✓	✓	✓	✓	IMPACT	✓	✓	—	—	—	—
Ylmén et al.	[40]	2017	Sweden	Apartment	✓	✓	✓	✓	✓	EnergyPlus; Heat 3; Therm	✓	✓	—	—	—	✓
Braulio-Gonzalo et al.	[41]	2017	Spain	Generic envelope	✓	✓	✓	✓	✓	HULC	✓	✓	—	—	—	✓
Pomponi et al.	[42]	2017	UK	Generic envelope	✓	✓	✓	✓	✓	MATLAB; OpenLCA	✓	✓	—	—	—	✓
Bonomo et al.	[43]	2017	Undefined	Building Integrated Photovoltaic façade	—	✓	✓	✓	—	Excel	—	—	—	—	—	✓
Ashouri et al.	[44]	2016	Undefined	Generic envelope	✓	✓	✓	✓	✓	MATLAB	✓	✓	—	—	—	✓
Azari et al.	[45]	2016	USA	Office building	✓	✓	✓	✓	✓	Athena Impact Estimator; ANN	✓	✓	—	—	—	✓

\* The input values are: weather data (Wd), geometric dimensions (Gd), material properties (Mp), energy standards (En), and life cycle emissions (Lce). \*\* The output values are: embodied emission (Ee), operational energy (Oe), solar irradiation (Irr), and daylight factor (Df).

Recently, the use of parametric tools has also been adopted for the calculation of a number of other performance aspects in addition to solar radiation, such as the emissions from operational energy use and embodied emissions of materials [31–33]. Some studies led to the development of new methodologies that allow multi-objective optimization for energy and/or environmental assessments [34,35]. Nevertheless, to develop a parametric approach to conduct fast and simplified LCA analyses during the early stage of the design process is critical for ZEB designs. In this regard, Hollberg implemented an algorithm in Grasshopper to conduct LCA studies on a building's components [36]. However, it did not allow for a free control of the building's shape but only a minimal control was possible through few parameters, such as the number of levels and the building footprint.

### 2.3. Solar Irradiation at Different Latitudes

Nordic and Mediterranean climate zones largely differ due to the available solar irradiance and the annual sun path's distribution. The Scandinavian region has been considered, for a long time, an area characterized by a low solar potential compared to Central Europe. Nevertheless, recent studies demonstrated that some of these common assumptions were incorrect [46]. Jones and Underwood [47] presented the data collected by two sun tracking systems installed in Piteå (Sweden) and Freiburg (Germany) and the results proved that they receive almost the same annual global solar irradiation [46,48], although the distribution through the year is different. Those studies documented the growing interest in solar energy exploitation in the Scandinavian countries, and in this regard, the research carried out by Lobaccaro et al. [49] and Imenes et al. [50] is worth being mentioned.

In this paper, the weather data collected in Oslo (OS) (Norway) were chosen as representative of the Nordic climate zone. Oslo is classified according to the Köppen–Geiger classification as a “Warm Summer Continental Climate”. However, Oslo is located on the very edge of this climate area and it is characterized by some regular snow during winter with an average annual temperature of 6.7 °C. For the Mediterranean area, characterized by larger available solar irradiation, the sun path shows higher values of the azimuth angle compared to the Scandinavian region. The solar irradiation incident on a horizontal surface is higher, although the daylight hours throughout the year are almost the same, according to the monitoring campaign conducted by Castaldo et al. [51]. The city of Perugia (PG) (Italy) has been set as the location for the Mediterranean climate zone. The city belongs to the climate zone classified as “Cfb—Marine West Coast Climate” according to the Köppen–Geiger climate classification [52].

## 3. Methodology

### 3.1. Multi-Objective Optimization Workflow

This paper presents a workflow based on an algorithm defined through Grasshopper (Figure 1). Grasshopper is a parametric design tool based on Python scripts. It allows the implementation of different algorithms for parametric design by means of a visual programming interface. In this study, an algorithm implemented in a previous study [35] was used to parametrically control the building's volume of a ZEB Base Case (presented in Section 2.2). The algorithm allows conducting both solar irradiation analysis and environmental impact calculation to optimize the building's shape according to two objective functions: (i) maximization of the solar irradiation ( $Irr_{gi}$ ) harvesting on the building envelope and (ii) minimization of the embodied emissions ( $E_e$ ) due to the employed building's materials. The calculations are performed for all the design configurations. The inputs and outputs data, and the tools used to control the geometry (Gm) in each step of the workflow are shown in Table 2.

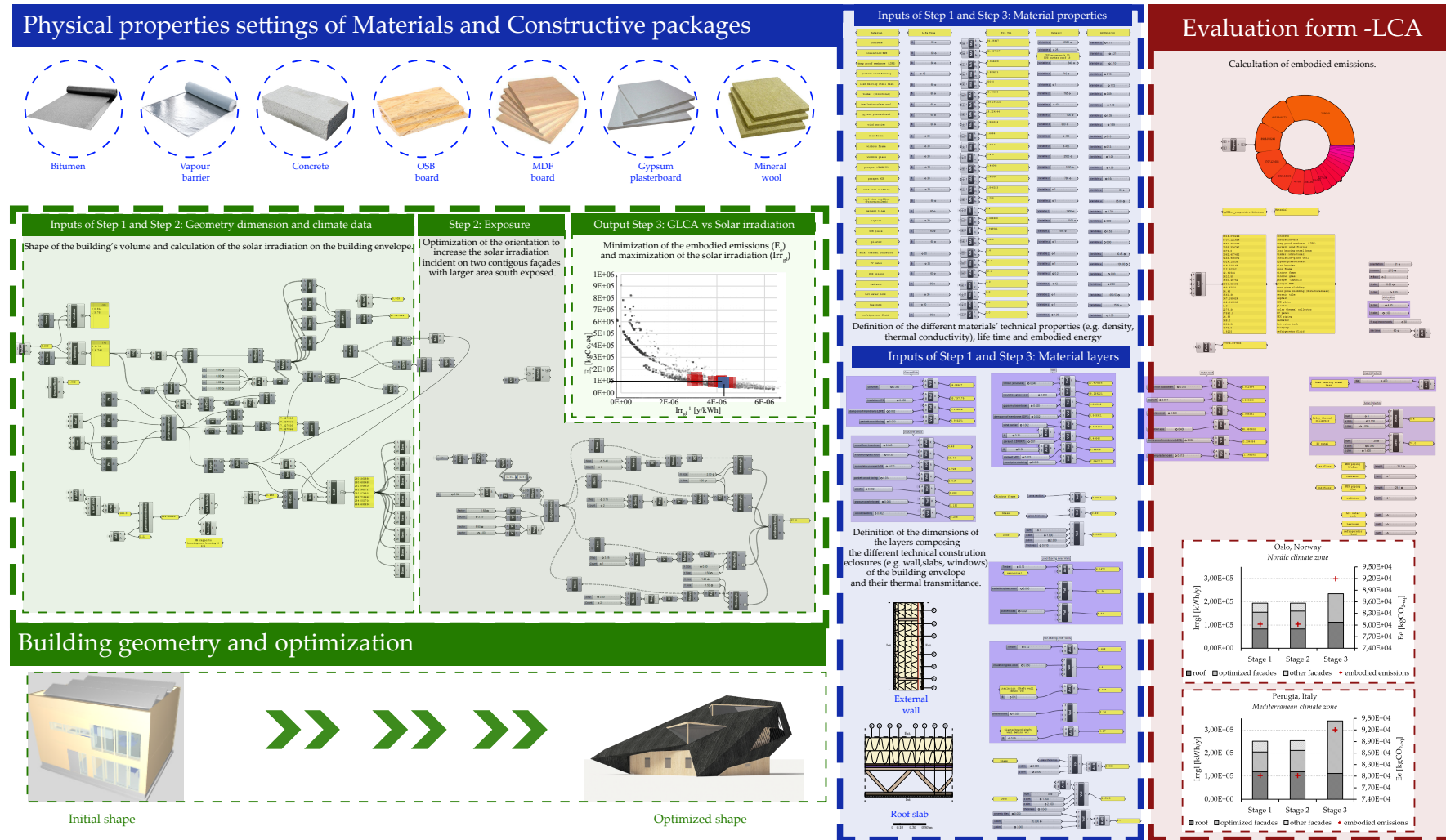


Figure 1. Overview of the algorithm developed in the Grasshopper environment with the different steps, inputs, and outputs.

Table 2. Overview of the workflow.

	Step 1					Step 2					Step 3				
<b>Inputs</b>	-	-	-	-	-	-	-	-	-	-	-	-	-	-	-
	Geometric dimensions	Material properties	Material layers	Climate data	Geographical information	Geometric dimensions	Climate data	Geographical information			Shape's control points	Material properties	Material layers	Climate data	Geographical information
<b>Workflow</b>	<b>Geometry</b> Shape of the building's volume and calculation of the solar irradiation on the building envelope					<b>Exposure</b> Optimization of the orientation to increase the solar irradiation incident on two contiguous façades					<b>LCA vs. Solar Irradiation</b> Minimization of the embodied emissions ( $E_e$ ) and maximization of the solar irradiation ( $Irr_{gl}$ )				
<b>Outputs</b>	Parametric 3D model and analyses of data and visualizations					Optimized exposure with a larger area south exposed					Optimized energy and environmentally responsive model				
<b>Tools and Analysis</b>	✓	✓	✓	-	-	✓	-	✓	✓	-	✓	✓	✓	-	✓
	Gm	$E_e$	$Irr_{gl}$	-	-	Gm	$E_e$	$Irr_{gl}$	-	-	Gm	$E_e$	$Irr_{gl}$	-	-
	Grasshopper	Evaluate for Gh	Ladybug	Galapagos	Octopus	Grasshopper	Evaluate for Gh	Ladybug	Galapagos	Octopus	Grasshopper	Evaluate for Gh	Ladybug	Galapagos	Octopus

The workflow is based on an algorithm that applies parametric transformations to evaluate the solar and environmental optimization of the building shape in the early design stage. It is structured in three steps.

In *Step 1*, the *Base Case* was modeled through a parametric approach followed by the calculation of the building's materials' embodied emissions, and the global solar irradiation on the envelope. The *Evaluation component* of Grasshopper was used to conduct the GHG analysis in terms of embodied emissions for each model configuration. This made it possible to control several material properties to evaluate the impact of the materials and technologies on the building's total embodied emissions. The system boundaries used for the GHG analysis are defined according to EN 15804; specifically, the stages A1–A5, B4, and B6 have been used. Stage B4 (replacement of building components) was applied only to the PV system, which has a service life of 30 years (Table 3).

According to the Norwegian Standard 3940:2012 [53], the building lifetime was set to 60 years, while the functional unit, used for referring to the energy and environmental impact, is 1 m<sup>2</sup> of HFA. The emission factors of the building materials were retrieved from the Norwegian Environmental Product Declarations (EPD) ([www.epd-norge.no](http://www.epd-norge.no)) when possible, or alternatively, the information was collected from the *Ecoinvent 3.0* LCA database. The emission factors were integrated in the algorithm with the other parameters specifically developed to control the variation of the building's geometry and components. In fact, *Step 1* of the GHG analysis is strictly connected to the building's geometry: the volumes and the masses of the employed building materials were estimated and constantly updated during the optimization process; then, they were converted into carbon emissions by using the emission factors. The GHG emissions of the technical installations (heat pump, boiler, radiator, etc.) were calculated by multiplying the number of technical components by the emission factors of each component. A third cluster of parameters was introduced in Grasshopper to calculate the annual global solar irradiation incident on the building's envelope. This solar irradiation analysis was carried out by using the *Ladybug* plug-in. Iterative grid-based analyses visualized in radiation maps were

performed by setting “r-trace” parameters in Radiance (Table 4) in accordance with similar previous studies [54].

**Table 3.** Building life cycle phases according to [55].

Product Stage			Construction Process Stage			Use Stage					End-of-Life				Benefits and Loads Beyond the System Boundaries					
A1	A2	A3	A4	A5	B1	B2	B3	B4	B5	B6	B7	C1	C2	C3	C4	D1	D2	D3	D4	
Raw material supply	Transport	Manufacturing	Transport	Construction installation process	Use	Maintenance	Repair	Replacement	Refurbishment	Operational energy use (space heating)	Operational energy use (appliances)	Operational water use	Deconstruction demolition	Transport	Water processing	Disposal	Reuse	Recovery	Recycling	Exported energy/potential

**Table 4.** Set of “r-trace” parameters.

Ambient Bounces	Ambient Divisions	Ambient Super Samples	Ambient Resolution	Ambient Accuracy	Specular Threshold	Direct Sampling	Direct Relays
3	1000	20	300	0.10	0.15	0.20	2

Two different weather files—the .epw files of Perugia (Italy) and Oslo (Norway)—were used as inputs to define reference values for the *Base Case*, which are later compared to the optimized configurations carried out from *Step 3*.

In *Step 2*, the orientation of the ZEB *Base Case* model and the exposure of its façades were optimized to increase the south exposed area for the installation of the building-integrated photovoltaic (BiPV) panels. Such an optimization process aims to develop a configuration with the highest incident solar irradiation on two contiguous façades by varying the building’s orientation and façades’ exposure. The box-shaped dwelling (the *Base Case*) was rotated by 90° by incremental angle steps of 1 degree. The optimization was conducted by coupling *Ladybug* with the Galapagos evolutionary solver to generate the optimized configurations in terms of global incident solar irradiation on two contiguous façades (fitness). The optimization process starts by creating an initial population of the optimized building orientation and façades’ exposure through multiple-crossovers mutations and with random combinations of genes. The best solutions according to the fitness criteria (i.e., highest solar irradiation on two contiguous façades) are selected. Then, the process is repeated. The optimization process runs until the final population of optimized building shapes has been generated. The analysis was conducted on both the Mediterranean and the Nordic climate zones.

In *Step 3*, the parametric transformations of the *Base Case*’s shape were introduced in the workflow. The shape’s variations represent the core of this part of the work, in which parametric design principles are applied. In fact, the shape configuration of the *Base Case* is controlled through few control points, whose geometrical positions were moved to find a balance between the maximization of solar irradiation on the building envelope and the minimization of the embodied emissions. Both of them (solar irradiation and embodied emissions) were set as objective functions (fitness) of the evolutionary solver Octopus. Differently from Galapagos, Octopus allows the optimization of several objective

functions simultaneously within a single process. The investigated processes were progressively reported on a Cartesian plan, whose axes indicate  $E_e$  and  $Irr_{gl}^{-1}$ . The mathematical inverse function allowed obtaining a better arrangement of the solutions by locating the best ones close to the origin of the axes. Finally, the comparison between the optimized building shape for the Nordic and the Mediterranean climate zones has been performed.

### 3.2. The ZEB Single-Family House Case Study

The process was applied to a single-family house pilot project in Oslo (Norway) that aims to reach the zero environmental impact in terms of embodied and operational emissions by reducing its energy consumptions (passive approach) and applying efficient energy production strategies (active approach). This concept building, largely described in previous works [56], was used as the *Base Case* in this study (Figure 2a). The building is a typical Norwegian single-family house and it is arranged in two stories. The building volume is a box shape with a rectangular plan of 10 by 8 m. The longest façades are exposed respectively towards north and south. The house contains four bedrooms and two bathrooms (Figure 2b,c) with a total heated floor area (HFA) of 160 m<sup>2</sup>.

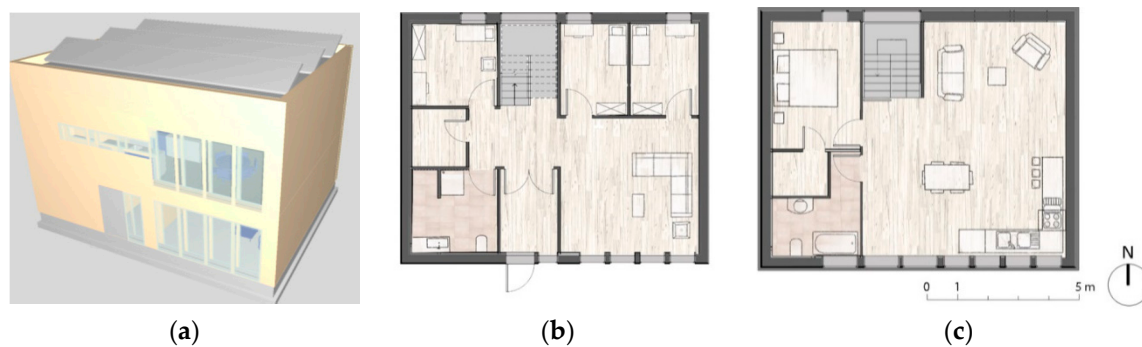


**Figure 2.** View of the zero-emission building (ZEB) *Base Case* (a), plans of the ground floor (b), and the first floor (c).

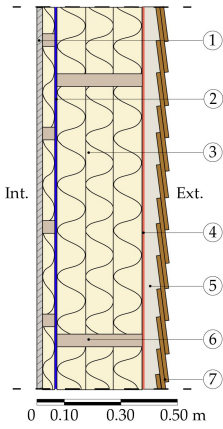
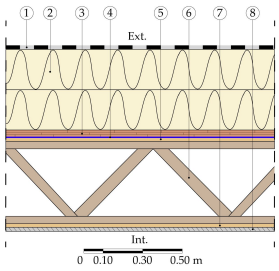
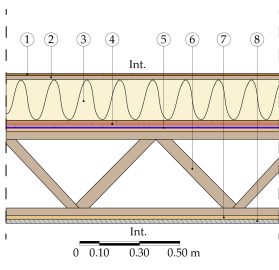
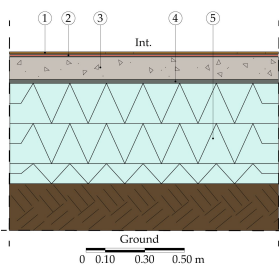
The embodied emissions for the construction materials are listed in Table 5, while the characteristics of the construction of the *Base Case* are detailed in Table 6.

The energy requirements are achieved by an air-to-water heat pump integrated with solar collectors on the façade and with a PV system installed on the flat roof. The used module is from the manufacturer SunPower (SPR-3333NE-WHT-D), and it is a monocrystalline cell type with high efficiency (around 20%). The energy production due to the 8.3 m<sup>2</sup> of ST has been calculated equal to 3300 kWh/y, while the 69 m<sup>2</sup> of the PV system allows it to reach more than 11,000 kWh/y.

**Table 5.** Building elements of the ZEB *Base Case* included in the LCA calculation [35].

Building Elements	GHG Emissions [kgCO <sub>2-eq</sub> /m <sup>2</sup> HFA Year]
Groundwork and foundations	1.44
Superstructure and outer walls	1.69
Inner walls	0.50
Structural deck	0.24
Outer roof	0.64
Heating distribution system and units	0.65
Ventilation system	0.05
Photovoltaic system	2.90
Solar thermal system	0.24
<b>Total</b>	<b>8.35</b>

**Table 6.** Thermal transmittance value (U-value) of the different building envelope components of the ZEB Base Case.

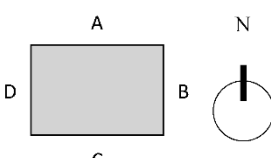
Element	U—Value [W/m <sup>2</sup> K]	Composition
External wall	0.12	<p>Timber-frame wall with 350-mm-thick insulation</p> <p><i>Indoor</i></p> <ol style="list-style-type: none"> <li>Gypsum plasterboard (15 mm)</li> <li>Wind barrier (0.2 mm)</li> <li>Mineral wool (350 mm) (0.2 mm)</li> <li>Vapor barrier (PE-foil)</li> <li>Vertical timber structure (30 mm)</li> <li>Horizontal timber structure (50 mm)</li> <li>Wood pine cladding (15 mm)</li> </ol> <p><i>Outdoor</i></p> 
Roof	0.10	<p>Compact roof with 400-mm-thick insulation</p> <p><i>Outdoor</i></p> <ol style="list-style-type: none"> <li>Asphalt (15 mm)</li> <li>Mineral wool (400 mm)</li> <li>MDF board (30 mm)</li> <li>Damp-proof membrane (LPDE 0.2 mm)</li> <li>OSB board (15 mm)</li> <li>Wooden trusses (h: 300 mm)</li> <li>OSB board (15 mm)</li> <li>Gypsum plasterboard (15 mm)</li> </ol> <p><i>Indoor</i></p> 
Internal Slab	-	<p><i>Indoor</i></p> <ol style="list-style-type: none"> <li>Parquet wood flooring (15 mm)</li> <li>MDF board (15 mm)</li> <li>Mineral wool (200 mm)</li> <li>OSB board (15 mm)</li> <li>Damp-proof membrane (LPDE 0.2 mm)</li> <li>Wooden trusses (h: 300 mm)</li> <li>OSB board (15 mm)</li> <li>Gypsum plasterboard (15 mm)</li> </ol> <p><i>Indoor</i></p> 
Slab on the ground	0.07 (0.06) The value in brackets considers the thermal resistance of the ground.	<p>Slab on the ground with 500-mm-thick insulation.</p> <p><i>Indoor</i></p> <ol style="list-style-type: none"> <li>Parquet wood flooring (15 mm)</li> <li>PE foil (0.2 mm)</li> <li>Concrete slab (100 mm)</li> <li>Radon membrane (0.2 mm)</li> <li>EPS (500 mm)</li> </ol> <p><i>Ground/Soil</i></p> 
Windows	0.65	Triple-glazed low-energy windows, with insulated frame
Doors	0.65	Insulated doors

## 4. Results and Discussion

### 4.1. Step 1, ZEB Reference Model

The embodied emissions of the materials for the *Base Case* were calculated to be equal to 8.35 kgCO<sub>2-eq</sub>/m<sup>2</sup> HFA per year (80,200 kgCO<sub>2-eq</sub>, total emissions for 60 years). The global solar incident irradiation on the building envelope was estimated equal to around 194,000 kWh/y in Oslo, while it reached around 250,000 kWh/y in Perugia. In Table 7, the global solar incident irradiation on each façade is reported, as well as its average value on the whole envelope. Already at the early stage, the results highlight how the geographical location can affect the distribution of solar irradiation on the building envelope.

**Table 7.** Results of the solar analyses conducted during *Step 1* on the ZEB concept model.

ZEB Concept Model					
Weather file	Oslo		Perugia		
	kWh/y	%	kWh/y	%	
North façade (A)	13,700	7	16,000	6	
East façade (D)	24,700	13	30,900	12	
South façade (C)	48,200	25	54,800	22	
West façade (B)	24,100	12	30,900	12	
Roof	83,200	43	119,100	47	
Total Irr <sub>gl</sub>	kWh/y	194,000		250,000	
Average Irr <sub>gl</sub>	kWh/m <sup>2</sup> y	560		730	

It is worth noting that the lower solar angles in the Nordic region led to a slightly minor irradiation of the roof—only 43% in Oslo against 47% in Perugia—counterbalanced by the increment of the south exposed façade—25% in Oslo against 22% in Perugia. The percentages refer to the annual total global irradiation (Total Irr<sub>gl</sub>) of the two single cases.

### 4.2. Step 2, Exposure Optimization of the Box-Shaped Model

The optimization performed in *Step 2* demonstrated that the box-shaped model of the *Base Case* could be more efficient if rotated by 51° (Tables 8 and 9). Although the total annual global irradiation does not change significantly among the three investigated orientations, the solar energy incident on two contiguous façades—in this case, façade B and façade C (Table 7)—increases by 12% if compared to the 90° rotated model in both climate zones. The algorithm allowed designing a model in which up to 40% of the solar energy is incident on the two contiguous façades B and C. In particular, the solar irradiation incident on façades B and C is equal to 77,400 kWh/y in the Nordic case study, while the Mediterranean achieves 91,900 kWh/y.

**Table 8.** Optimization performed by the Galapagos evolutionary solver on solar analyses in *Step 2*.

Rotation Angle/Exposure	Weather File	0°/Biggest Façade Oriented to South		51°/Two Contiguous Façades Oriented to South		90°/Smallest Façade Oriented to South	
		Oslo	Perugia	Oslo	Perugia	Oslo	Perugia
Façade A	kWh/y	13,700	16,000	19,900	25,200	30,300	37,900
Façade B	kWh/y	24,700	30,900	36,300	42,400	39,300	44,700
Façade C	kWh/y	48,200	54,800	41,100	49,600	29,600	37,900
Façade D	kWh/y	24,100	30,900	14,000	17,800	11,100	13,100
Roof	kWh/y	83,200	119,100	83,200	119,100	83,200	119,100
Façades B and C	kWh/y	72,900	85,800	77,400	91,900	68,900	82,600
Total Irr <sub>gl</sub>	kWh/y	193,900	251,700	194,500	254,100	193,500	252,700
Average Irr <sub>gl</sub>	kWh/m <sup>2</sup> y	560	730	570	740	560	740

**Table 9.** Advantages and disadvantages of optimization performed by the Galapagos evolutionary solver on solar analyses in *Step 2*.

	<p><b>0°/Biggest façade oriented to south</b></p> <ul style="list-style-type: none"> <li>- <i>Advantages:</i> maximum façade’s area facing south where there is the highest amount of solar irradiation.</li> <li>- <i>Disadvantages:</i> higher variation of total solar irradiation on the different façades</li> </ul>
	<p><b>90°/Smallest façade oriented to south</b></p> <ul style="list-style-type: none"> <li>- <i>Advantages:</i> lower variation of the total solar irradiation on the different façades.</li> <li>- <i>Disadvantages:</i> minimum façade’s area facing to the south</li> </ul>
	<p><b>51°/Two contiguous façades oriented to south</b></p> <ul style="list-style-type: none"> <li>- <i>Advantages:</i> the highest amount of solar irradiation on two contiguous façades. Therefore, the higher façade’s area can be irradiated.</li> <li>- <i>Disadvantages:</i> the other two façades received the lowest incoming irradiation.</li> </ul>

4.3. Step 3, Towards a Responsive ZEB

The outcomes from *Step 2* were used as inputs in *Step 3*, where the ZEB’s shape was modified from the initial box model of the *Base Case*.

The Octopus evolutionary solver performed a series of iterative assessments that allowed to develop the most environmentally optimal configurations characterized by the lowest impact in terms of embodied emissions from materials. All building configurations are depicted in the graphs reported in Figure 3.

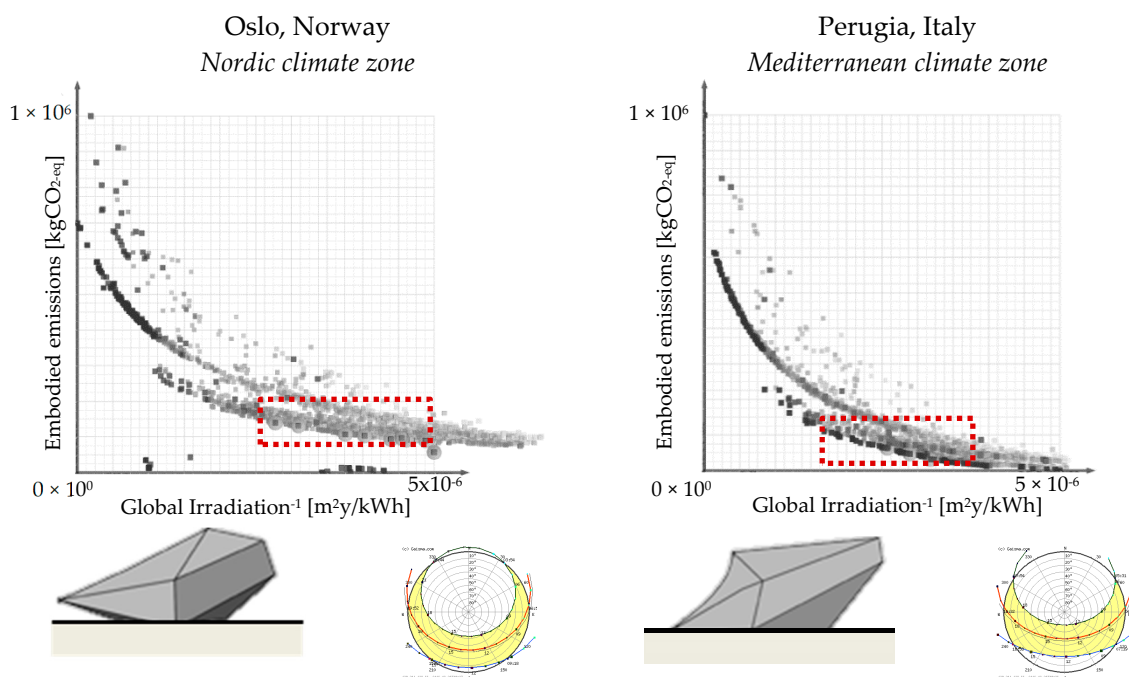


**Figure 3.** Step 3—graphical representation of the outcomes of the multi-objective optimization.

Among those, the two configurations on the bottom (area delimited by the red dashed line in Figure 3) are those best fitting the curve (maximization of solar irradiation on the building envelope and minimization of the embodied emissions). The tilted angles of the main surfaces highlighted how the designed concepts are influenced by the sun paths. The height of the sun at noon in Oslo changes significantly during the year, where it varies from around 55° in the summer to below 10° in the winter.

Differently, the sun height at noon in Perugia varies from 25° in the winter to 70° in the summer. Such a variance of the angles of incidence of solar irradiation during the year shaped the building differently. In fact, while in the Mediterranean climate zone the optimized configuration appears flatter—the main surfaces are characterized by the same tilt angles, about 40° from the horizontal direction—in the Nordic zone, the building envelope of the model turns out to be as vertical as possible—the tilt angles range from 40° to more than 60°.

Figure 3 shows the graphical representation of the outcomes of the multi-objective optimization. The area delimited by the red dashed line included the most optimized configurations designed in Step 3. In fact, the others were characterized by a too high level of embodied emissions or by a shape too flat for being considered dwellings. The optimized volumes and the sun paths used on the process are shown on the bottom of Figure 3. Therefore, as summarized in Table 10, the annual global solar irradiation on the selected optimized shapes varies from 234,500 in Oslo to 339,000 kWh/y in Perugia. The developed algorithm allowed achieving a 20% improvement of solar irradiation in the Nordic climate zone and 35% in the Mediterranean area. This has been achieved by both improving the model's orientation, façades' exposure, and incrementing the envelope's surface area—a factor that penalizes the solar irradiation per square meter compared to Step 2—while maintaining as low as possible the materials' embodied emissions. The embodied emissions were estimated equal to 92,000 kgCO<sub>2-eq</sub> for both the optimized configurations: these are 15% higher than those calculated for the reference *Base Case*. The higher embodied emissions may be/are compensated by both the lower energy requirements for heating and the higher efficiency of the PV panels.

**Table 10.** Optimization performed by the Octopus evolutionary solver on solar analysis in Step 3.

Weather File/Location	Optimized Shape			
	Oslo		Perugia	
	kWh/y	kWh/m <sup>2</sup> y	kWh/y	kWh/m <sup>2</sup> y
<b>Façades</b>	122,600	335	227,500	415
<b>Roof</b>	111,800	110	111,500	80
<b>Total Irr<sub>gl</sub></b>	234,400	445	339,000	495

#### 4.4. The Evolutionary Process

The evolutionary process described in this paper and the achieved results have demonstrated the suitability of the parametric design approach to maximize the exploitation of the available solar energy on the ZEB concept model in different climate zones. As highlighted in Figure 4, the magnitude of the enhancement is influenced by the latitude, but even in adverse climates such as the Nordic one, the algorithm allowed to achieve a significant improvement from the *Base Case*. At the beginning of the study, the concept of the *Base Case* model located in Oslo was characterized by an incident solar irradiation equal to 194,000 kWh/y, which was increased to 234,400 kWh/y at the end of Step 3. A significant goal was also achieved in Step 2, in which the solar irradiation on two south exposed contiguous façades was increased by 12%. Regarding the ZEB optimized in the Mediterranean zone, the solar irradiation reached 339,000 kWh/y from the initial 251,700 kWh/y. Furthermore, in this case, the optimization conducted in Step 2 allowed to improve the exposure of the best two contiguous façades by 12%. When it came to GHG analysis, the embodied emissions were equal to 80,200 kgCO<sub>2-eq</sub> in Step 1 and Step 2, and such an amount increased to 92,000 kgCO<sub>2-eq</sub> at the end of Step 3 in both

the climate zones. This increment is caused by the greater envelope's extension in the optimized configurations if compared to the *Base Case*.

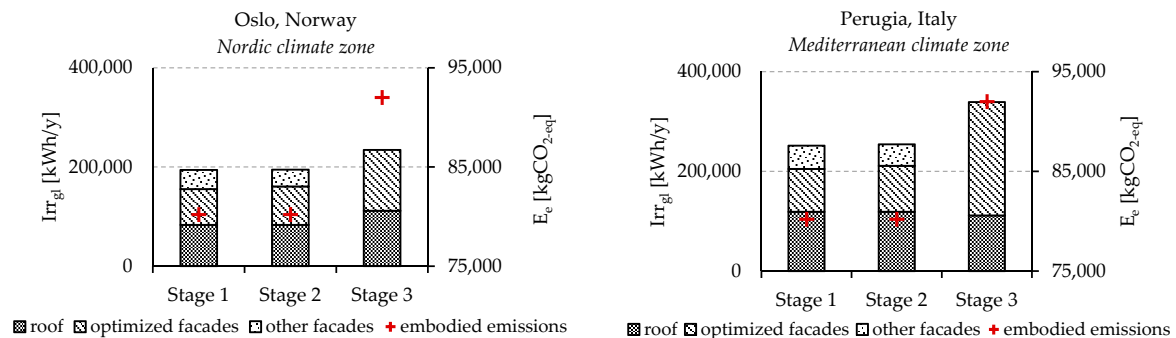


**Figure 4.** Trend and values of global solar incident irradiation and emissions embodied in materials throughout the optimization process about Oslo and Perugia. In both *Step 1* and *Step 2*—box-shaped model—the exposure of two contiguous façades was optimized. In *Step 3*, the whole envelope was enhanced, thus the graphs report a null value for the bar of “other façades”.

#### 4.5. Limitations of the Study

It should be noted that the ZEB *Base Case* was originally designed as a generic concept model for the local climatic conditions of Oslo, and the building was considered a detached house without any urban surroundings. It is relevant to underline that the urban context affects the optimization process and the optimal configuration of the environmentally responsive layout and building volume. The urban context may reduce solar accessibility and the solar energy production. In this respect, the presence of other buildings may affect both the positions and geometry of the solar systems integrated on the building envelope as demonstrated in previous studies regarding the influence of urban complexity and density on solar accessibility and PV localizations [57,58].

Finally, the assessment of the building's energy performances during the operational stage has not been investigated in this paper, as further and detailed analyses regarding this aspect represent part of future developments. The optimized configurations carried out from the optimization process have been slightly adjusted to maintain the original HFA.

## 5. Conclusions and Future Developments

This work proposes a possible application of the parametric design principles to the development of a ZEB optimized in terms of solar energy potential and embodied emissions due to materials. The proposed methodology finalized to buildings form-finding was developed in the Grasshopper environment: the algorithm integrates the component for conducting environmental analyses (Evaluate component) with the one for energy assessment (*Ladybug*). Finally, Galapagos and Octopus tools were used as evolutionary solvers. This workflow enables an iterative analysis by dynamically linking each parameter and simultaneously modeling and comparing numerous building configurations. Furthermore, the Grasshopper tool allows visualizing in real-time the optimized model's layouts from the early design stages, and the related data about annual global solar irradiation and embodied emissions.

The results demonstrated how the algorithm—and the parametric design principles in general—can be considered suitable for ZEB design and optimization. In fact, the solar irradiation caught by the envelope turned out to be increased by up to 35% in the Mediterranean climate zone, with a low variation of embodied emissions that could be fully compensated by the advantages derived from the optimized exposure (low energy requirements for heating, PV plant's efficiency higher than 20%). Similarly, the ZEB base case located in the Nordic climate zone showed an increment of the  $Irr_{gl}$  as high as 20% at the end of *Step 3*.

The main achievements are summarized as follows:

- The optimization process of the orientation (*Step 2*) allows increasing the  $Irr_{gl}$  by 12% in both the Nordic and Mediterranean climate zones;
- The multi-objective optimization from *Step 3* led to increase the  $Irr_{gl}$  by 20% in the Nordic zone and 35% in the Mediterranean zone;
- The  $E_e$  estimated at the end of *Step 3* was increased by a share of 15%.

The proposed innovative workflow and the early results derive from its application in different climate zones. However, there are some future developments which are still under investigation and should allow a better assessment of the optimized models. Furthermore, the operational stage could be introduced in the calculation to have a complete view of the ZEB concept model and to better understand the effect of the optimization process on the whole life cycle of the building. To achieve those goals, the design of the building cannot be interrupted at the preliminary investigation stage of shape and volume, but it would be necessary to go further by arranging the rooms and defining their functions.

**Author Contributions:** Conceptualization, G.L. and M.M.; methodology, G.L., M.M. and N.L.; software, M.M.; formal analysis, M.M.; investigation, M.M. and G.L.; resources, G.L., M.M. and N.L.; data curation, M.M.; writing—original draft preparation, G.L., M.M. and N.L.; writing—review and editing, G.L., M.M., N.L. and R.A.B.; visualization, M.M.; supervision, G.L. All authors have read and agreed to the published version of the manuscript.

**Funding:** This research received no external funding and the APC was funded by Norwegian University of Science and Technology—Trondheim (Norway).

**Acknowledgments:** The authors wish to thank the Norwegian University of Science and Technology (Trondheim, Norway) and the University of Perugia (Perugia, Italy) for having supported the collaboration between the two universities in this work, framed by the EU programme for education, training, youth and sport—ERASMUS+. The authors gratefully acknowledge the support from the Research Council of Norway and several partners through the Research Centre on Zero Emission Buildings.

**Conflicts of Interest:** The authors declare no conflict of interest.

## Nomenclature

### Variables

Irr	Solar irradiation
E	Emissions
HFA	Heated Floor Area
U	Thermal transmittance

### Subscripts

gl	Global
e	Embodied

### Acronyms

GHG	Greenhouse Gas
IPCC	Intergovernmental Panel on Climate Change
RES	Renewable Energy Source
NZEB	Net zero-energy buildings
ZEB	Zero-Emission Building
IEA	International Energy Agency
SHC	Solar Heating and Cooling
LCA	Life Cycle Assessment
PV	Photovoltaic
ST	Solar Thermal
ZESH	Zero-Emissions Solar House
OS	Oslo
PG	Perugia
Gm	Geometry
EPD	Environmental Product Declaration
BiPV	Building-Integrated Photovoltaic

## References

1. Pachauri, R.K.; Meyer, L.A. *Climate Change 2014: Synthesis Report. Contribution of Working Groups I, II and III to the Fifth Assessment Report of the Intergovernmental Panel on Climate Change*; Pachauri, R.K., Meyer, L.A., Eds.; IPCC: Geneva, Switzerland, 2014; ISBN 978-92-9169-143-2.
2. American National Standards Institute. *Energy Standard for Building Except Low-Rise Residential Buildings*; ASHRAE: Atlanta, GA, USA, 2013.
3. Berardi, U. A cross-country comparison of the building energy consumptions and their trends. *Resour. Conserv. Recycl.* **2017**, *123*, 230–241. [[CrossRef](#)]
4. European Parliament and Council Directive 2010/31/EU of the European Parliament and of the Council of 19 May 2010 on the Energy Performance of Buildings 2010. Available online: <https://eur-lex.europa.eu/legal-content/EN/ALL/?uri=CELEX%3A32010L0031> (accessed on 18 September 2020).
5. European Commission. Communication from the Commission to the European Parliament, the Council, the European Economic and Social Committee and the Committee of the Regions—Energy Roadmap 2050. 2011. Available online: <https://eur-lex.europa.eu/LexUriServ/LexUriServ.do?uri=COM:2011:0885:FIN:EN:PDF> (accessed on 18 September 2020).
6. Berardi, U. ZEB and nZEB (Definitions, Design Methodologies, Good Practices, and Case Studies). 2018. Available online: [https://www.researchgate.net/publication/325258523\\_ZEB\\_and\\_nZEB\\_definitions\\_design\\_methodologies\\_good\\_practices\\_and\\_case\\_studies](https://www.researchgate.net/publication/325258523_ZEB_and_nZEB_definitions_design_methodologies_good_practices_and_case_studies) (accessed on 18 September 2020).
7. Pless, S.; Torcellini, P. *Net-Zero Energy Buildings: A Classification System Based on Renewable Energy Supply Options*; National Renewable Energy Laboratory: Golden, CO, USA, 2010.
8. Torcellini, P.; Pless, S.; Deru, M.; Crawley, D. *Zero Energy Buildings: A Critical Look at the Definition*; National Renewable Energy Laboratory: Golden, CO, USA, 2006.
9. Garde, F.; Ayoub, J.; Aelenei, L.; Aelenei, D.; Scognamiglio, A. *Solution Sets for Net Zero Energy Buildings: Feedback from 30 Buildings Worldwide*; John Wiley & Sons: Hoboken, NJ, USA, 2017; ISBN 9783433604663.
10. Voss, K.; Musall, E. *Net Zero Energy Buildings—International Projects on Carbon Neutrality in Buildings*; Walter de Gruyter: Berlin, Germany, 2011.
11. Donn, M.; Garde, F. *Solution Sets and Net Zero Energy Buildings: A Review of 30 Net ZEBs Case Studies Worldwide*; John Wiley & Sons: New York, NY, USA, 2014.
12. Cho, J.; Shin, S.; Kim, J.; Hong, H. Development of an energy evaluation methodology to make multiple predictions of the HVAC&R system energy demand for office buildings. *Energy Build.* **2014**, *80*, 169–183. [[CrossRef](#)]
13. Athienitis, A.; O'Brien, W. *Modeling, Design, and Optimization of Net-Zero Energy Buildings*; Ernst & Sohn: Berlin, Germany, 2015.
14. Marszal, A.J.; Heiselberg, P.; Bourrelle, J.S.; Musall, E.; Voss, K.; Sartori, I.; Napolitano, A. Zero Energy Building—A review of definitions and calculation methodologies. *Energy Build.* **2011**, *43*, 971–979. [[CrossRef](#)]
15. Cellura, M.; Guarino, F.; Longo, S.; Mistretta, M. Energy life-cycle approach in Net zero energy buildings balance: Operation and embodied energy of an Italian case study. *Energy Build.* **2014**, *72*, 371–381. [[CrossRef](#)]
16. Hernandez, P.; Kenny, P. From net energy to zero energy buildings: Defining life cycle zero energy buildings (LC-ZEB). *Energy Build.* **2010**, *42*, 815–821. [[CrossRef](#)]
17. Lund, H.; Marszal, A.; Heiselberg, P. Zero energy buildings and mismatch compensation factors. *Energy Build.* **2011**, *43*, 1646–1654. [[CrossRef](#)]
18. Mohajeri, N.; Upadhyay, G.; Gudmundsson, A.; Assouline, D.; Kämpf, J.; Scartezzini, J.-L. Effects of urban compactness on solar energy potential. *Renew. Energy* **2016**, *93*, 469–482. [[CrossRef](#)]
19. International Energy Agency. *Technology Roadmap: Solar Photovoltaic Energy 2014*; International Energy Agency: Paris, France, 2014.
20. International Energy Agency. *World Energy Outlook 2019*; International Energy Agency: Paris, France, 2019.
21. Pajek, L.; Košir, M. Implications of present and upcoming changes in bioclimatic potential for energy performance of residential buildings. *Build. Environ.* **2018**, *127*, 157–172. [[CrossRef](#)]
22. Raza, M.Q.; Nadarajah, M.; Ekanayake, C. Demand forecast of PV integrated bioclimatic buildings using ensemble framework. *Appl. Energy* **2017**, *208*, 1626–1638. [[CrossRef](#)]
23. Khambadkone, N.K.; Jain, R. A bioclimatic analysis tool for investigation of the potential of passive cooling and heating strategies in a composite Indian climate. *Build. Environ.* **2017**, *123*, 469–493. [[CrossRef](#)]

24. Ulpiani, G.; Giuliani, D.; Romagnoli, A.; di Perna, C. Experimental monitoring of a sunspace applied to a NZEB mock-up: Assessing and comparing the energy benefits of different configurations. *Energy Build.* **2017**, *152*, 194–215. [[CrossRef](#)]
25. Finocchiaro, L.; Lobaccaro, G. Bioclimatic Design of Green Buildings. In *Handbook of Energy Systems in Green Buildings*; Springer: Berlin/Heidelberg, Germany, 2017; pp. 1–31. ISBN 978-3-662-49088-4.
26. Pignataro, M.A.; Lobaccaro, G.; Zani, G. Digital and physical models for the validation of sustainable design strategies. *Autom. Constr.* **2014**, *39*, 1–14. [[CrossRef](#)]
27. Oliveira, C.T.; Antonio, F.; Burani, G.F.; Udaeta, M.E.M. GHG reduction and energy efficiency analyses in a zero-energy solar house archetype. *Int. J. Low Carbon Technol.* **2017**, *12*, 225–232. [[CrossRef](#)]
28. Yi, Y.K.; Malkawi, A.M. Optimizing building form for energy performance based on hierarchical geometry relation. *Autom. Constr.* **2009**, *18*, 825–833. [[CrossRef](#)]
29. Lobaccaro, G.; Chatzichristos, S.; Leon, V.A. Solar Optimization of Housing Development. *Energy Procedia* **2016**, *91*, 868–875. [[CrossRef](#)]
30. Zani, A.; Tagliabue, L.C.; Poli, T.; Ciribini, A.L.C.; De Angelis, E.; Manfren, M. Occupancy Profile Variation Analyzed through Generative Modelling to Control Building Energy Behavior. *Procedia Eng.* **2017**, *180*, 1495–1505. [[CrossRef](#)]
31. Kiss, B.; Szalay, Z. Modular approach to multi-objective environmental optimization of buildings. *Autom. Constr.* **2020**, *111*, 103044. [[CrossRef](#)]
32. Soflaei, F.; Shokouhian, M.; Tabadkani, A.; Moslehi, H.; Berardi, U. A simulation-based model for courtyard housing design based on adaptive thermal comfort. *J. Build. Eng.* **2020**, *31*, 101335. [[CrossRef](#)]
33. Adeli, M.M.; Farahat, S.; Sarhaddi, F. Parametric analysis of a zero-energy building aiming for a reduction of CO<sub>2</sub> emissions for warm climate. *Environ. Sci. Pollut. Res.* **2020**, *27*, 34121–34134. [[CrossRef](#)]
34. Lolli, N.; Fufa, S.M.; Inman, M. A Parametric Tool for the Assessment of Operational Energy Use, Embodied Energy and Embodied Material Emissions in Building. *Energy Procedia* **2017**, *111*, 21–30. [[CrossRef](#)]
35. Lobaccaro, G.; Wiberg, A.H.; Ceci, G.; Manni, M.; Lolli, N.; Berardi, U. Parametric design to minimize the embodied GHG emissions in a ZEB. *Energy Build.* **2018**, *167*, 106–123. [[CrossRef](#)]
36. Hollberg, A.; Ruth, J. LCA in architectural design—A parametric approach. *Int. J. Life Cycle Assess* **2016**, *21*, 943–960. [[CrossRef](#)]
37. Cavalliere, C.; Hollberg, A.; Dell’Osso, G.R.; Habert, G. Consistent BIM-led LCA during the entire building design process. In *IOP Conference Series: Earth and Environmental Science*; IOP Publishing Ltd: Bristol, UK, 2019; Volume 323, p. 12099. [[CrossRef](#)]
38. Ramin, H.; Hanafizadeh, P.; Ehterami, T.; AkhavanBehabadi, M.A. Life cycle-based multi-objective optimization of wall structures in climate of Tehran. *Adv. Build. Energy Res.* **2019**, *13*, 18–31. [[CrossRef](#)]
39. Azzouz, A.; Borchers, M.; Moreira, J.; Mavrogianni, A. Life cycle assessment of energy conservation measures during early stage office building design: A case study in London, UK. *Energy Build.* **2017**, *139*, 547–568. [[CrossRef](#)]
40. Ylmén, P.; Mjörnell, K.; Berlin, J.; Arfvidsson, J. The influence of secondary effects on global warming and cost optimization of insulation in the building envelope. *Build. Environ.* **2017**, *118*, 174–183. [[CrossRef](#)]
41. Braulio-Gonzalo, M.; Bovea, M.D. Environmental and cost performance of building’s envelope insulation materials to reduce energy demand: Thickness optimisation. *Energy Build.* **2017**, *150*, 527–545. [[CrossRef](#)]
42. Pomponi, F.; D’Amico, B. Holistic study of a timber double skin façade: Whole life carbon emissions and structural optimisation. *Build. Environ.* **2017**, *124*, 42–56. [[CrossRef](#)]
43. Bonomo, P.; Frontini, F.; De Berardinis, P.; Donsante, I. BIPV: Building envelope solutions in a multi-criteria approach. A method for assessing life-cycle costs in the early design phase. *Adv. Build. Energy Res.* **2017**, *11*, 104–129. [[CrossRef](#)]
44. Ashouri, M.; Astaraei, F.R.; Ghasempour, R.; Ahmadi, M.H.; Feidt, M. Optimum insulation thickness determination of a building wall using exergetic life cycle assessment. *Appl. Therm. Eng.* **2016**, *106*, 307–315. [[CrossRef](#)]
45. Azari, R.; Garshasbi, S.; Amini, P.; Rashed-Ali, H.; Mohammadi, Y. Multi-objective optimization of building envelope design for life cycle environmental performance. *Energy Build.* **2016**, *126*, 524–534. [[CrossRef](#)]
46. Boström, T. Solar Power Plants in the North. Available online: <https://www.nordicenergy.org/project/solar-power-plants-in-the-north/> (accessed on 6 July 2020).

47. Jones, A.D.; Underwood, C.P. A thermal model for photovoltaic systems. *Sol. Energy* **2001**, *70*, 349–359. [[CrossRef](#)]
48. Klitkou, A.; Godoe, H. The Norwegian PV manufacturing industry in a Triple Helix perspective. *Energy Policy* **2013**, *61*, 1586–1594. [[CrossRef](#)]
49. Lobaccaro, G.; Carlucci, S.; Croce, S.; Paparella, R.; Finocchiaro, L. Boosting solar accessibility and potential of urban districts in the Nordic climate: A case study in Trondheim. *Sol. Energy* **2017**, *149*, 347–369. [[CrossRef](#)]
50. Imenes, A.G.; Kanters, J. 3D solar maps for the evaluation of building integrated photovoltaics in future city districts: A norwegian case study. In Proceedings of the 2016 IEEE 43rd Photovoltaic Specialists Conference (PVSC), Portland, OR, USA, 5–10 June 2016; pp. 3141–3146.
51. Castaldo, V.L.; Pisello, A.L.; Pigliautile, I.; Piselli, C.; Cotana, F. Microclimate and air quality investigation in historic hilly urban areas: Experimental and numerical investigation in central Italy. *Sustain. Cities Soc.* **2017**, *33*, 27–44. [[CrossRef](#)]
52. Kottek, M.; Grieser, J.; Beck, C.; Rudolf, B.; Rubel, F. World Map of the Köppen-Geiger climate classification updated. *Meteorol. Z.* **2006**, *15*, 259–263. [[CrossRef](#)]
53. NS 3940:2012 Calculation of the Areas and Volumes of Buildings. Standards Norway, Oslo, Norway. Available online: <https://www.standard.no/en/PDF/FileDownload/?redir=true&filetype=Pdf&preview=true&item=529401&category=5> (accessed on 22 September 2020).
54. Reinhart, C.F.; Wienold, J. The daylighting dashboard—A simulation-based design analysis for daylight spaces. *Build. Environ.* **2011**, *46*, 386–396. [[CrossRef](#)]
55. EN 15978:2011 EN 15978. Sustainability of Construction Works. Assessment of Environmental Performance of Buildings. Calculation Method 2011. 2011. Available online: <https://infostore.saiglobal.com/preview/is/en/2011/i.s.en15978-2011-lc-2011-11.pdf?sku=1500481> (accessed on 18 September 2020).
56. Houlihan Wiberg, A.; Georges, L.; Dokka, T.H.; Haase, M.; Time, B.; Lien, A.G.; Mellegård, S.; Maltha, M. A net zero emission concept analysis of a single-family house. *Energy Build.* **2014**, *74*, 101–110. [[CrossRef](#)]
57. Nault, E.; Peronato, G.; Rey, E.; Andersen, M. Review and critical analysis of early-design phase evaluation metrics for the solar potential of neighborhood designs. *Build. Environ.* **2015**, *92*, 679–691. [[CrossRef](#)]
58. Kanters, J.; Wall, M. A planning process map for solar buildings in urban environments. *Renew. Sustain. Energy Rev.* **2016**, *57*, 173–185. [[CrossRef](#)]



© 2020 by the authors. Licensee MDPI, Basel, Switzerland. This article is an open access article distributed under the terms and conditions of the Creative Commons Attribution (CC BY) license (<http://creativecommons.org/licenses/by/4.0/>).